

Range Image Segmentation and Surface Parameter Extraction for 3-D Object Recognition of Industrial Parts *

Joonhee Han, Richard A. Volz, and Trevor N. Mudge

Robotics Research Laboratory
Department of Electrical Engineering and Computer Science
The University of Michigan, Ann Arbor, MI 48109

Abstract

This paper addresses the problem of extracting certain types of surfaces for 3-dimensional object recognition in the presence of partial occlusion and noise using range information. We restrict consideration to man made industrial parts. In this case, we need only work with a small set of surface shapes such as planes, cylinders, and spheres since such shapes are common in industrial parts and it is only necessary to recognize and locate a sufficient set of surface regions to uniquely distinguish the part being observed from all others that might be present. We describe a way of extracting the parameters of these types of surfaces using normal analysis. The use of surface parameters then allows efficient and robust use of a matching process for object recognition and pose determination even though there are many undefined or occluded surface regions.

1 Introduction

As a branch of vision, range image analysis has received great attention due to the direct geometrical information it provides, and recent improvement of the speed and the accuracy of range imaging systems[20]. For the most part, however, the input models of the objects under study have been restricted to a small set of surface types or features in order to reduce the computation time or memory space required, or to simplify the analysis. For example, [7,8,11] used sparse data, while [11,12,15] concentrated on using only edges or occluding boundaries. In other cases, simple surfaces such as planes have been reconstructed for more reliable and accurate analysis[1,3,5,6,10, 11,14,15,18]. In this case objects were modeled or approximated as polyhedrons.

In more sophisticated techniques that can handle curved

surfaces, certain sets of quadric surfaces have been extracted[1,6,9,13,14,18] and represented in terms of the quadric equation. None of these representations can describe the general objects without approximation. While it is theoretically possible to perform a higher level analysis by extracting quadric parameters and using those parameters in matching, in our experience, the parameters extracted from the coefficients in the quadric equation are very sensitive to noise in the original image. For more general objects, a range image segmentation method has been proposed using local curvature information[2]. However, in this case no higher level processing for matching was proposed.

We observe that it is not necessary to work with a set of surface shapes large enough to describe the entire surface of a large number of parts. It is sufficient to work with a subset of all surface types which are present in adequate proportion to allow recognition and pose estimation. In a man made environment, a small set of surface types like planes, cylinders, and spheres, constitute the majority of surfaces of objects[4], and thus make a reasonable set of surfaces to be examined. Several methods of extracting planes and (a subset of) quadric surfaces have been studied. Optimization and eigenvalue analysis[1,6], quadric invariants[9], modified Hough transforms[16], or modified Hough transform with multiple computation with several window sizes[13] have been used to classify different types of surfaces. Eigenvalues or quadric invariants are good discriminators in a mathematical sense, but, in a computational sense, are often too sensitive to noise and quantization errors.

Rather than use quadric parameters or eigenvalues, we calculate the geometric properties of a sufficient set of shapes, planes, cylinders and spheres, to allow recognition in the presence of occlusion and noise. The calculations are based upon an analysis of the surface normals. We also work with entire regions in the image rather than small patches in order to encompass enough of the curved surfaces to allow us to extract reliable estimates of the parameters. Our approach uses a mixture of histogram-

* This work was supported by the Army Research Office under grant no. DOD-C-DAAG29-84-K-0070.

ming and parameter fitting to obtain good estimates. The techniques are also amenable to efficient processing on a parallel computer structure such as a hypercube. In this paper, we address primarily the issue of extracting defined surfaces and their features out of several undefined regions in an image.

2 Overview of segmentation procedure

The system uses range images and models of the possible parts as inputs and produces a list of (object identity, object pose) pairs as an output. There are two basic parts to the system, a low level subsystem that segments the range image into regions of like surface type and determines the surface parameters for these regions, and a high level subsystem that uses the surface parameters in a matching scheme for object recognition and pose determination. In this paper, however, we discuss only the low level process.

We first calculate the normal vectors of the image points using a simple operator. In the vicinity of jump boundaries, the normal vectors are not defined and the simple operator used yields very large values of the x or y-directional component, and z directional normal values near zero. Thus, the jump boundaries can be found by thresholding the z directional normals. Planes are detected by histogram analysis of their normal vectors, and parameters of planes and their regions are determined. The jump boundaries or planar regions are then used to segment the remaining regions. We apply a surface finding process to these and extract cylinders and spheres. These regions and their parameters are also recorded. The surface finding process is a complex system of cross products, projections, histogramming and parameter fitting which we describe in the next two sections.

3 Normals and surface equations

We can represent the depth values in a range image as a function of x and y coordinates, $z = g(x, y)$, where g is of type C^1 except at jump boundaries and at a certain internal boundaries. In this section we describe a method of calculating surface normals that will be used in segmentation of different types of surfaces, and we also show the relations between the normals and the surface equations.

3.1 Surface normal

If a surface can be represented by a function which has derivatives within a certain boundary, the normal can be calculated within the boundary. Let $z(x, y) = g(x, y)$. In

our coordinate system, z axis comes out of the paper. In a small neighborhood of a point (x, y) , we assume that $g(x, y)$ is C^1 . Then the unit normal $\mathbf{N} = \mathbf{N}(x, y)$ can be calculated by the equation,

$$\mathbf{N}(x, y) = \frac{\nabla g(x, y)}{\|\nabla g(x, y)\|} \quad (1)$$

where ∇ represents the gradient operator. Since we assumed $g(x, y)$ is C^1 , first order Taylor approximations can be made within a small boundary around the point (x, y) . In this case, the first order equations describe a plane. If \mathbf{x} is a point on the plane, then $\mathbf{x} \cdot \mathbf{N} = d$, where d is a constant, $ax + by + cz = d$ for some a, b , and c . If $c = 0$ we can never observe the plane. Hence there are only three independent parameters, a, b , and d , and we normalize c to unity. Then the plane equation can be represented as $ax + by + z = d$, or $z = g(x, y) = -ax - by + d$. The constants a and b can be found by the equation,

$$-a = \frac{\partial g(x, y)}{\partial x} = \lim_{\Delta x \rightarrow 0} \frac{g(x + \Delta x, y) - g(x, y)}{\Delta x}$$

and,

$$-b = \frac{\partial g(x, y)}{\partial y} = \lim_{\Delta y \rightarrow 0} \frac{g(x, y + \Delta y) - g(x, y)}{\Delta y}$$

Then an approximation to a is,

$$-a(i, j) = z(i + 1, j) - z(i, j)$$

Since this calculation is noise sensitive, we modify the operator so that it reduces the noise sensitivity by averaging the value in nine locations around (i, j) , i.e., $(i - 2, j)$, $(i - 1, j - 1)$, $(i - 1, j + 1)$, $(i, j - 2)$, (i, j) , $(i, j + 2)$, $(i + 1, j - 1)$, $(i + 1, j + 1)$, and $(i + 2, j)$. Let $\alpha_{i,j} = 1/2\{z(i - 1, j) - z(i + 1, j)\}$. Then the x-directional normal is calculated by,

$$N_x = \frac{1}{9}(\alpha_{i-2,j} + \alpha_{i-1,j-1} + \alpha_{i-1,j+1} + \alpha_{i,j-2} + \alpha_{i,j} + \alpha_{i,j+2} + \alpha_{i+1,j-1} + \alpha_{i+1,j+1} + \alpha_{i+2,j}) \quad (2)$$

The y-directional normal can be calculated similar way. Then the unit normal is $(N_x/s, N_y/s, 1/s)^t$, where $s = \sqrt{N_x^2 + N_y^2 + 1}$. N_z is considered positive in every case. An interesting characteristic of this operator is that it is simple to calculate and proper for high speed computation (5 by 7 convolution). Another point is that if applied on jump boundary, it gives large value of s , making z directional values small. Hence it can be applied to any region including jump boundaries, and can be used in detecting jump boundaries.

3.2 Surface equations, normals and parameters

In this section we will use the surface normals to derive equations of planes, cylinders, spheres, and cones.

Let $f(x, y, z) = 0$ be the equation of the surface. Then $\mathbf{N} = [N_x \ N_y \ N_z]^t = \nabla f / \|\nabla f\|$ is a normal vector from a point of a surface.

1. Plane: A plane is a set of points that satisfies $\mathbf{N} \cdot \mathbf{x} = d$, where \mathbf{x} is a point on a surface, and d is a constant. Two planes with the same normals and different d can only be connected by a jump boundary.

2. Sphere: A spherical surface can be determined by four parameters: radius, and the center of the sphere which has three parameters. The relationships between the radius r , the normal \mathbf{N} , the center \mathbf{c} can be represented by the equation, $(\mathbf{x} - \mathbf{c})^t(\mathbf{x} - \mathbf{c}) = r^2$, where, $\mathbf{c} = (x_0 \ y_0 \ z_0)^t$. If we expand it,

$$f(x, y, z) = x^2 + y^2 + z^2 - 2(xx_0 + yy_0 + zz_0) + x_0^2 + y_0^2 + z_0^2 - r^2$$

From $\mathbf{N} = \nabla f / \|\nabla f\|$, we have,

$$r\mathbf{N} - \mathbf{x} + \mathbf{c} = \mathbf{0} \quad (3)$$

3. Cylindrical surface : For the moment, assume that the axis passes through the origin of the coordinate system. Then, the equation of the surface can be represented as follows(see fig. 1).

$$\begin{aligned} \|\mathbf{x} - (\mathbf{x} \cdot \mathbf{u})\mathbf{u}\|^2 &= r^2 \\ (\mathbf{x} - (\mathbf{x} \cdot \mathbf{u})\mathbf{u})^t(\mathbf{x} - (\mathbf{x} \cdot \mathbf{u})\mathbf{u}) &= \mathbf{x}^t\mathbf{x} - \mathbf{x}^t\mathbf{u} - \mathbf{u}^t\mathbf{x} \\ &= \mathbf{x}^t(\mathbf{I} - \mathbf{u}\mathbf{u}^t)\mathbf{x} = r^2 \end{aligned}$$

where \mathbf{I} is a 3 by 3 identity matrix, $\mathbf{u} = (u_1, u_2, u_3)^t$ is a unit directional vector of the axis of the cylinder, and r is the radius of the cylinder. The normal at each point of the cylindrical surface is,

$$\mathbf{N} = \frac{\nabla f}{\|\nabla f\|} = \frac{1}{r} \begin{pmatrix} (1 - u_1^2)x + u_1u_2y + u_1u_3z \\ u_1u_2x + (1 - u_2^2)y + u_2u_3z \\ u_1u_3x + u_2u_3y + (1 - u_3^2)z \end{pmatrix}$$

or, in vector representation,

$$r\mathbf{N} = (\mathbf{I} - \mathbf{u}\mathbf{u}^t)\mathbf{x} \quad (4)$$

If the axis of the cylinder does not pass the origin of the coordinate system, there is a translation vector \mathbf{x}_0 . In this case \mathbf{x} is replaced by $\mathbf{x} - \mathbf{x}_0$ in the above equations.

4. Conic surface : The parameters of cones are, the location of the peak, \mathbf{x}_0 , the direction of the axis, \mathbf{u} , and the angle between the axis and the line passing the peak and one point on the surface of the cone, θ . Let $k = \tan(\theta)$. Then, as we can see from figure 2,

$$\{\mathbf{x} - (\mathbf{x} \cdot \mathbf{u})\mathbf{u}\}^t(\mathbf{x} - (\mathbf{x} \cdot \mathbf{u})\mathbf{u}) = k^2\{(\mathbf{x} \cdot \mathbf{u})\mathbf{u}\}^t\{(\mathbf{x} \cdot \mathbf{u})\mathbf{u}\}$$

After some manipulation we have ,

$$\begin{aligned} \mathbf{x}^t\mathbf{x} - 2(\mathbf{x}^t\mathbf{u})^2 + (1 - k^2)(\mathbf{x}^t\mathbf{u})^2 &= \mathbf{x}^t\mathbf{x} - (k^2 + 1)(\mathbf{x}^t\mathbf{u})^2 = 0 \\ f(x, y, z) &= (x^2 + y^2 + z^2) - (k^2 + 1)(xu_1 + yu_2 + zu_3)^2 = 0 \end{aligned} \quad (5)$$

If the vertex is located at \mathbf{x}_0 , then \mathbf{x} is replaced by $\mathbf{x} - \mathbf{x}_0$. The gradient of the equations are,

$$\begin{aligned} \nabla f_x &= 2x - 2(k^2 + 1)u_1(xu_1 + yu_2 + zu_3) = 2(x - awu_1) \\ \nabla f_y &= 2y - 2(k^2 + 1)u_2(xu_1 + yu_2 + zu_3) = 2(y - awu_2) \\ \nabla f_z &= 2z - 2(k^2 + 1)u_3(xu_1 + yu_2 + zu_3) = 2(z - awu_3) \end{aligned}$$

where $a = k^2 + 1$, and $w = \mathbf{x} \cdot \mathbf{u}$. The square of the magnitude of the gradient is,

$$\begin{aligned} \|\nabla f\|^2 &= \nabla f_x^2 + \nabla f_y^2 + \nabla f_z^2 \\ &= 4\{x^2 + y^2 + z^2 - 2aw(xu_1 + yu_2 + zu_3) + a^2w^2\} \\ &= 4\{x^2 + y^2 + z^2 + (a^2 - 2a)w^2\} \\ &= 4(k^2 + 1)k^2w^2 \end{aligned}$$

$$\|\nabla f\| = 2k(k^2 + 1)^{\frac{1}{2}}(xu_1 + yu_2 + zu_3)$$

and,

$$\mathbf{N} = \frac{\begin{bmatrix} x - (k^2 + 1)(\mathbf{x} \cdot \mathbf{u})u_1 \\ y - (k^2 + 1)(\mathbf{x} \cdot \mathbf{u})u_2 \\ z - (k^2 + 1)(\mathbf{x} \cdot \mathbf{u})u_3 \end{bmatrix}}{k(k^2 + 1)\mathbf{x} \cdot \mathbf{u}} \quad (6)$$

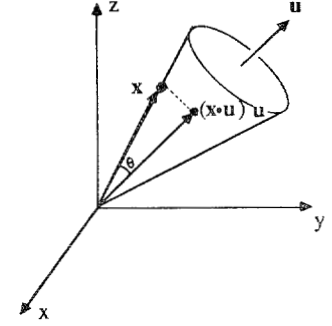
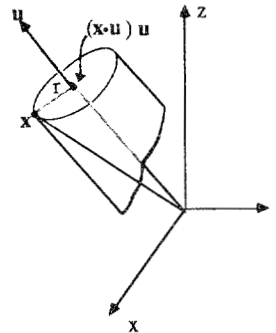


Figure 1: Cylindrical surface

Figure 2: Conic surface

4 Surface extraction and parameter calculation

After calculation of normals and determination of jump boundaries, surfaces are extracted in the order of planes, cylinders, spheres. We process the regions divided by jump boundaries or region boundaries that are extracted in the previous step. Extraction process stops when there

are no regions to be analyzed. The last remaining regions, if they exist, are either undefined regions that cannot be described by the defined surface types (within certain error threshold) or too small to calculate meaningful surface types.

4.1 Plane region extraction

Planes are easy to extract compared to other types of surfaces. But, in general, there are still numerical problems. For example, it is difficult to determine whether certain line segment is a part of a circle, part of a straight line, or neither of them.

The normals N_x and N_y of every pixel in range image are calculated using equation (2). The regions where $N_z \approx 0$ are classified as jump regions. In these regions, we cannot extract any type of regions correctly. Hence we exclude these regions from surface detection step. With the remaining region(s), we form a histogram of N_x . If there is a sizable plane, the histogram shows a peak. Usually there are several peaks. Among the several peaks we choose the highest peak, and find the values of the peak. Without noise there will be a single value. But in the presence of noise, there will be several high values around the correct value. To detect this, we smooth the histogram using a gaussian filter $h(x) = \frac{10}{\sqrt{2\pi}\sigma} e^{-x^2/2\sigma^2}$, where $\sigma = 5$. After smoothing, we detect two valleys around the peak. The peak value between the valleys is used and denoted P_x . Then we extract regions corresponding to the peak, and make a histogram of N_y of the region, and find the peak of histogram of N_y . There might be several regions whose normals belong to P_x , and P_y . Among these we choose the region in which the area is maximum, and calculate the parameters of the plane. If the size of the region is greater than some threshold, we extract the region and register plane parameters and the region. These steps are repeated until no further planes are extracted.

4.2 Cylindrical surface extraction

When the axis of the cylinder does not pass through the origin, equation (4) becomes, $r\mathbf{N} = (\mathbf{I} - \mathbf{u}\mathbf{u}^t)(\mathbf{x} - \mathbf{x}_0)$. The problems are to determine the parameters \mathbf{u} , \mathbf{x}_0 , and r , and to extract only the regions corresponding to the cylindrical surface.

First, we determine the direction of the axis using the normal vectors calculated in the earlier step. From the direction of the axis we determine a rotation matrix, \mathbf{R} , such that, $\mathbf{R}\mathbf{u} = (0, 0, 1)^t$. Using this rotation matrix we project data to a plane that is perpendicular to \mathbf{u} . By analyzing the projected data we determine the radius and the translation vector, \mathbf{x}_0 . We can also remove noncylindrical regions by analyzing the projected data. In the projection process we determine the two end points of the

axis in 3-D space.

Direction of axis

Every normal on the surface of a cylinder is perpendicular to the direction of the axis. If we choose two nonparallel normals on the surface, the cross product of the normals gives the direction of the axis. To overcome the effects of image noise, we perform the following steps.

1. For each pair of unit normals, \mathbf{n}_1 and \mathbf{n}_2 , $\mathbf{n}_1 \cdot \mathbf{n}_2 < T$, calculate cross product of the normals.
(T : a constant)
2. Make a histogram of the x directional vector of the cross product and find the maximum value.
3. Make a histogram of the y directional vector of the cross product and find the maximum value.
4. If steps 2, and 3 are successful, a candidate axis direction is determined. If not, next region is chosen to be analyzed.

The candidate axis direction is used in making the projection matrix. If some false peak was formed by non cylindrical regions, it will be detected in the projection or fitting step.

Projection of data

Once the candidate direction, \mathbf{u} , is known, we project the range values on the image to the surface that is perpendicular to the axis. The projection matrix \mathbf{R} maps sampled points on the surface of the cylinder onto the xy plane. That is, we develop the transformation matrix in such a way that the direction of axis \mathbf{u} is rotated to z axis in the transformed coordinates. If the direction of the axis is correct the projection of surface data to a plane will be an arc or a circle.

\mathbf{R} is a 3 by 3 orthonormal matrices, and has the property that $\mathbf{R}\mathbf{u} = (0, 0, 1)^t$. We assume that $u_1^2 + u_2^2 > 0$. There are several orthonormal matrix that satisfy the relationship. One matrix can be derived as follows,

$$\mathbf{R} = \begin{bmatrix} u_2/s & -u_1/s & 0 \\ u_1u_3/s & -u_2u_3/s & -s \\ u_1 & u_2 & u_3 \end{bmatrix} \quad (7)$$

where, $s = \sqrt{u_1^2 + u_2^2}$. By multiplying \mathbf{R} by surface points and taking only x and y components gives the cross section of the projection. From this cross section, which is 2-d circular arc if cylindrical region is projected, the center and radius can be calculated. If a non-cylindrical region is projected, this section shows other forms. By fitting circles, we can extract radius and center, or we can reject the data if insufficient data fits to a circle. Non cylindrical regions are rejected in this step. Two end points of the

cylinder, i.e the location of the cylinder is also calculated. Final refitting extracts only regions corresponding to the extracted parameters.

4.3 Spherical region extraction

For the remaining regions the strategy is to find out whether there are possible center points and radii. If the evidence is strong, the regions corresponding to the estimated parameters are extracted. This is similar to the general hough transform[16,20], but different in that the candidate center and radius are calculated by geometrical information and normal of a sphere. A histogram(or 1-dimensional accumulator) for each of the unknown parameters is needed.

In the presence of noise, we assume that the majority of the normal lines pass within a small neighborhood of the center. If we pick two points on the surface, the two normals may not meet at all. Hence, as a candidate center, we choose the center point of a line segment that is perpendicular to both of the normals. If the two normals meet, the candidate center is the meeting point.

Let \mathbf{m} and \mathbf{n} be the unit surface normals at points \mathbf{a} and \mathbf{b} respectively with $\mathbf{m} \neq \mathbf{n}$. The parametric form of the straight line through \mathbf{a} parallel to \mathbf{m} is the set of \mathbf{x} in E^3 which can be represented by $\mathbf{x} = k\mathbf{m} + \mathbf{a}$, where $-\infty < k < +\infty$.

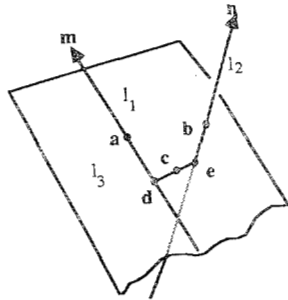


Figure 3:

Let l_1 and l_2 be two lines that pass through \mathbf{a} and \mathbf{b} with normals \mathbf{m} and \mathbf{n} respectively, and let l_3 is perpendicular to both l_1 and l_2 (fig 3). Then the direction of l_3 is given as $\mathbf{p} = \mathbf{m} \times \mathbf{n}$. We want to determine the center point of l_3 as the candidate point of the center of the sphere. The parametric equation of a plane through \mathbf{a} and parallel to both \mathbf{m} and \mathbf{p} is $\mathbf{x} = h\mathbf{m} + k\mathbf{p} + \mathbf{a}$, where, $-\infty < h < +\infty$, $-\infty < k < +\infty$. Let the point \mathbf{e} be the position where the plane and l_2 meet and let \mathbf{d} the point where line l_1 and l_3 meet. Since the parametric form of l_2 is $\mathbf{x} = i\mathbf{n} + \mathbf{b}$, $-\infty < i < +\infty$, at \mathbf{e} we have, $\mathbf{e} = h\mathbf{m} + k\mathbf{p} + \mathbf{a} = i\mathbf{n} + \mathbf{b}$, and $h\mathbf{m} - i\mathbf{n} + k\mathbf{p} = \mathbf{b} - \mathbf{a}$. Here the values of h, i, k are found by

$$[\mathbf{m}, -\mathbf{n}, \mathbf{p}] [h, i, k]^t = [\mathbf{b} - \mathbf{a}]$$

\mathbf{d} can be found in the same way, and the candidate point is estimated as $\frac{1}{2}(\mathbf{d} + \mathbf{e})$. Ideally the distances $\|\mathbf{a} - \mathbf{c}\|$ and $\|\mathbf{b} - \mathbf{c}\|$ are same, and they are equal to the radius. If either normal is incorrect, or one or both of the points \mathbf{a} and \mathbf{b} do not lie on the surface of the spherical region, the two distances are not likely to be close. To eliminate this case, the distances are tested. That is, if

$$1 - \alpha \leq \frac{\|\mathbf{a} - \mathbf{c}\|}{\|\mathbf{b} - \mathbf{c}\|} \leq 1 + \alpha$$

for some $0 < \alpha < \epsilon$, then the value of each component of \mathbf{c} is recorded. The candidate radius value $\frac{1}{2}(\|\mathbf{a} - \mathbf{c}\| + \|\mathbf{b} - \mathbf{c}\|)$ is recorded to the radius histogram. The process of finding candidate center and radius is performed for sampled pair of normals whose normalized inner product is less $1 - \epsilon$. If there exists a peak for each of the four histograms, a spherical region is extracted by refitting the data to the parameters.

5 Experimental results

In order to test the segmentation procedures described above, synthetically generated range images were used. For the tests reported here, gaussian noise with standard deviation of 2.0 was added to the depth values distributed from 0 to 255. The image sizes are 128 by 128 except for figure 7 which is 100 by 100. The surface plots of the range images are shown in figure 8. Good segmentation results are obtained as shown in figures 4, 5, 6, and 7. To reduce the computation, the program automatically adjusted to the size of the region in calculation, so the data used are more sparse than the actual image.

In figure 4 : A - A range image whose surface plot is shown in figure 8-a. This image consists only planes; B - The value of x-directional normals calculated by equation (2). The values of the normals are rescaled from 0(black) to 255(white) for display. Bold black lines correspond to the jump boundaries where z-component of the normal is less than a small threshold value; C - The value of y-directional normals; D - The value of z-directional normals. In figures C and D, dark bold lines also correspond to the jump boundaries where z-directional normal is small; E - An example of planar regions with the same normals; F - Another regions with the same normals; G - Segmented regions colored by different grey values. Each region has plane parameters(normal and distance from the origin of the coordinate system); H - Boundaries of the segmented regions.

In figures 5 and 6-E : A - A range image whose surface plot is shown in figure 8-b. This image consists of two

cylinders with different radius; B, C, and D - x, y, and z-components of surface normals respectively. In these figures black bold lines also represent jump boundaries; E - Calculated end points of axes (represented by small crosses) and location of the axes (lines between the two crosses) of two cylinders; F - Extracted two cylindrical regions whose axes are shown in E; G - Center and radius of the big cylinder with refined projected data; H - Segmented region boundaries; 6-E - Another example of cylindrical axis detected and superimposed on the range image.

In figure 6 : A - A range image whose surface plot is shown in figure 8-c; B, C, and D - x, y, and z-component of surface normals respectively; F - extracted planar regions; G - A spherical region with its center and radius shown as a cross; H - Boundaries of the segmented regions.

In figure 7 : A - A range image whose surface plot is shown in figure 8-d. This model consists of planar regions and a cylindrical region with a smoothly connected spherical region; B, C, and D - x, y, and z-components of the surface normals respectively; E - Calculated axis

of the cylindrical region; F - Extracted cylindrical region. This region is extracted from the combination of spherical region shown in figure G; G - A spherical region with its radius and center shown as a cross; H - Boundaries of the segmented regions.

6 Summary

We have shown surface parameter and region extraction methods based on a surface normal analysis. For calculation of surface normals, a simple normal operator was devised [equation (2)]. We utilized regions segmented by jump boundaries and plane regions which are robust surface types compared to other curved regions. The regions are then analyzed one at a time, subdividing them further as necessary. By using the full regions, we retain the maximum possible curved regions without taking patches; this increases the reliability of the method. This method can be utilized as the low level process of 3-dimensional industrial vision system.

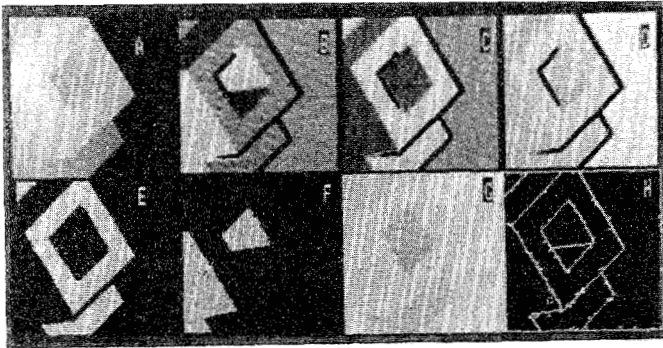


Figure 4:

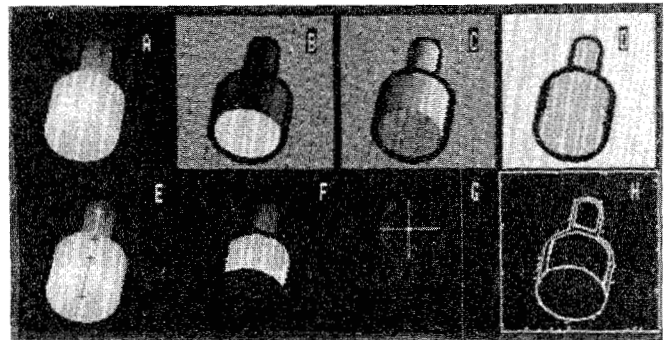


Figure 5:

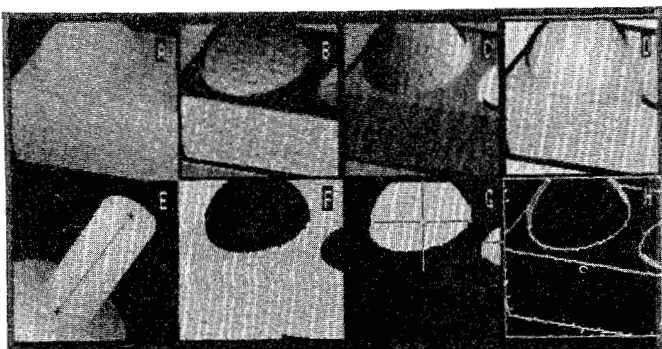


Figure 6:

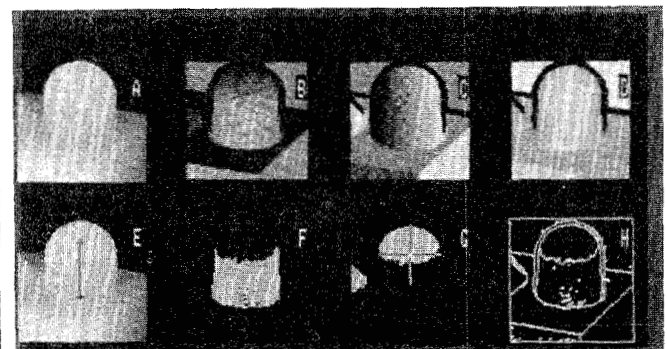


Figure 7:

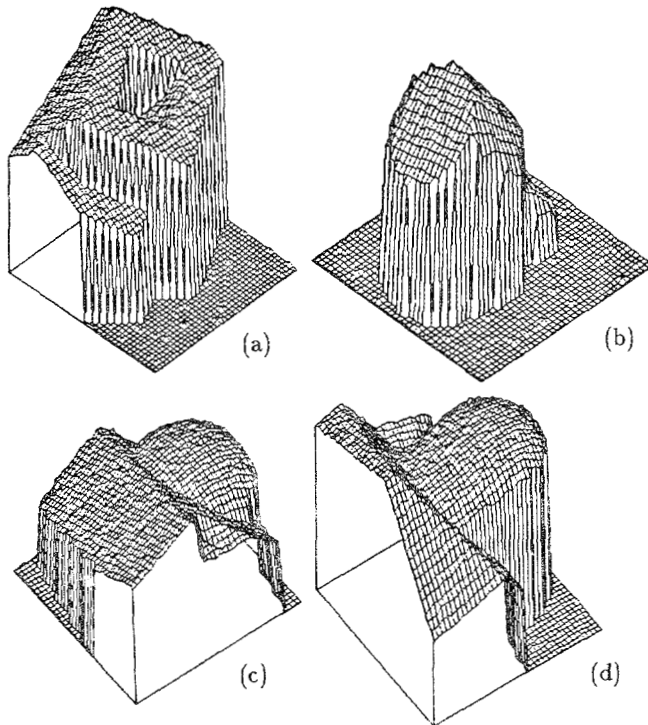


Figure 8:

References

- [1] N. Ayache, O. Faugeras, and B. Faverjon, "A Geometric Matcher for Recognizing and Positioning 3-D Rigid Objects," *SPIE Intelligent Robots and Computer Vision*, vol. 521, pp. 152-159.
- [2] Paul J. Besl and Ramesh C. Jain, "Segmentation Through Symbolic Surface Descriptions," *IEEE Proc. CVPR*, pp. 77-85, June 22-26, 1986.
- [3] Bir Bhanu, "Representation and Shape Matching of 3-D Objects," *IEEE Tran. on PAMI*, pp. 340-351, May 1984.
- [4] Ruud M. Bolle and David B. Cooper, "Bayesian Recognition of Local 3-D Shape by Approximating Image Intensity Functions with Quadric Polynomials," *IEEE Trans. on PAMI*, pp. 418-429, July 1984.
- [5] Richard O. Duda, David Nitzan, and Phyllis Barret, "Use of Range and Reflectance Data to Find Planar Surface Regions," *IEEE Trans. on PAMI*, July 1979.
- [6] O. D. Faugeras, "New Steps Toward a Flexible 3-D Vision System for Robotics," *Int'l Conference on Pattern Recognition*, vol. 2, pp. 796-805, July 30-August 2, 1984.
- [7] W. Eric L. Grimson and Tomas Lozano-Perez, "Model-Based Recognition and Localization from Sparse Range or Tactile Data," *The International Journal of Robotics Research*, vol. 3, no. 3, pp. 3-35, Fall 1984.
- [8] —, "Recognition and Localization of Overlapping Parts from Sparse Data in Two and three Dimensions," *IEEE International Conference on Robotics & Automation*, pp. 61-66, March 25-8, 1985.
- [9] E. L. Hall, J. B. K. Tio, C. A. McPherson, and F. A. Sadjadi, "Curved Surface Measurement and Recognition for Robot Vision," *IEEE 82 Conf. Industrial Application of Machine Vision*, pp. 187-192, 1982.
- [10] Thomas C. Henderson and Bir Bhanu, "Three Point Seed Method for the Extraction of Planar Faces from Range Data," *IEEE 1982 Conf. Industrial App. Machine Vision*, pp. 181-186, 1982.
- [11] M. Hebert and T. Kanade, "The 3-D Profile Method for Object Recognition," *IEEE Proc. CVPR*, pp. 458-463, June 19-13, 1985.
- [12] Patrice Horaud and Robert C. Bolles, "3DPO's Strategy for Matching Three-Dimensional Objects in Range Data," *IEEE Computer Society Int'l Conf. on Robotics*, pp. 78-85, March, 1984.
- [13] Xueyin Lin and William G. Wee, "Shape Detection Using Range Data," *IEEE International Conference on Robotics & Automation*, pp. 34-39, March 25-28, 1985.
- [14] —, "SDFS: A New Strategy for the Recognition of Object Using Range Data," *1986 IEEE Proc. International conf. Robotics and Automation*, pp. 770-775, April 7-10, 1986.
- [15] Michel J. Magee, Brian A. Boyer, Chiun-Hong Chien, and J. K. Aggarwal, "Experiments in Intensity Guided Range Sensing Recognition of Three-Dimensional Objects," *IEEE Transactions on Pattern Analysis and Machine Intelligence*, vol. PAMI-7, no. 5, pp. 629-637, November 1985.
- [16] Yolande Muller and Roger Mohr, "Planes and Quadrics Detection using Hough Transform," *7th International conference on Pattern Recognition*, pp. 1101-1103, July 30- Aug. 2, 1984.
- [17] Ramakant Nevatia and Thomas O. Binford, "Description and Recognition of Curved Objects," *Artificial Intelligence*, vol. 8, pp. 77-98, 1977.
- [18] Masaki Oshima and Yoshiaki Shirai, "Object Recognition Using Three Dimensional Information," *IEEE Trans. PAMI*, vol. PAMI-5, no. 4, July 1983.
- [19] David B. Shu, C. C. Li, and Y. N. Sun, "An Approach to 3-D Object Identification Using Range Images," *1986 IEEE Proc. International conf. Robotics and Automation*, pp. 118-125, April 7-10, 1986.
- [20] R. A. Jarvis, "A Perspective on Range Finding Techniques for Computer Vision," *IEEE Trans. on PAMI*, pp. 122-139, March 1983.